© 2021. Published by The Company of Biologists Ltd | Development (2022) 149, dev199694. doi:10.1242/dev.199694

RESEARCH REPORT

Retinal ganglion cell survival after severe optic nerve injury is modulated by crosstalk between Jak/Stat signaling and innate immune responses in the zebrafish retina

Si Chen[1,2,3], Kira L. Lathrop[2,4], Takaaki Kuwajima[2,5,*] and Jeffrey M. Gross[2,5,*]

ABSTRACT

Visual information is transmitted from the eye to the brain along the optic nerve, a structure composed of retinal ganglion cell (RGC) axons. The optic nerve is highly vulnerable to damage in neurodegenerative diseases, such as glaucoma, and there are currently no FDA-approved drugs or therapies to protect RGCs from death. Zebrafish possess remarkable neuroprotective and regenerative abilities. Here, utilizing an optic nerve transection (ONT) injury and an RNA-seq-based approach, we identify genes and pathways active in RGCs that may modulate their survival. Through pharmacological perturbation, we demonstrate that Jak/Stat pathway activity is required for RGC survival after ONT. Furthermore, we show that immune responses directly contribute to RGC death after ONT; macrophages/microglia are recruited to the retina and blocking neuroinflammation or depleting these cells after ONT rescues survival of RGCs. Taken together, these data support a model in which crosstalk between macrophages/microglia and RGCs, mediated by Jak/Stat pathway activity, regulates RGC survival after optic nerve injury.

KEY WORDS: Jak/Stat, RGC, Innate immune system, Neuroprotection, Zebrafish

INTRODUCTION

Visual information is transmitted from the eye to the brain along the optic nerve (ON), a structure composed of retinal ganglion cell (RGC) axons. The ON is highly vulnerable to damage and is compromised after acute injury and in neurodegenerative diseases, such as glaucoma. In glaucoma, RGC axons are the initial site of injury; this causes the RGCs to die and ultimately results in irreversible loss of visual function. Neuroprotective strategies for glaucoma treatment seek to maintain the health of RGCs even after axons have been damaged, or to prevent initial damage to the RGC axon itself (Almasieh et al., 2012; Chang and Goldberg, 2012). There has been substantial progress in identifying the molecular and cellular events that lead to RGC death in the glaucomatous eye (Almasieh et al., 2012; Chang and Goldberg, 2012; Syc-Mazurek and Libby, 2019); however, no FDA-approved therapies currently exist to protect RGCs from death. This highlights the need for new neuroprotective strategies that preserve RGCs during glaucoma or after acute ocular trauma.

Most RGCs die in mammals suffering from glaucoma or acute ocular trauma. For example, in mouse, ∼65% of RGCs are lost within 7 days of optic nerve injury (ONI), and >90% by 28 days (Li et al., 2020). Mammals are also unable to regenerate RGCs after ONI, leading to irreparable vision loss. Unlike mammals, zebrafish possess remarkable neuroprotective and regenerative capacity in the central nervous system (Cigliola et al., 2020; Lahne et al., 2020). When the ON is damaged by crush or transection, zebrafish mount a robust regenerative response and regenerate RGC axons, restoring visual connections and function (Diekmann et al., 2015). Moreover, it has been reported that ∼75% of zebrafish RGCs are protected from death after ONI, even up to 7-weeks post-injury (Zou et al., 2013), but the mechanisms underlying neuroprotection are unknown. With an interest in developing novel strategies to preserve RGCs during glaucoma and other trauma, we identify potential neuroprotective factors/pathways in zebrafish that mediate RGC survival after ONI.

RESULTS AND DISCUSSION

Zebrafish retain the majority of RGCs after ONT

To enable isolation of RGCs after injury, we first verified that GFP remained expressed in RGCs of adult *isl2b*:GFP fish (Pittman et al., 2008). In retinal cryosections, *isl2b*:GFP cells were detected in the ganglion cell layer (GCL), where they co-labeled with DAPI and the RGC-specific marker zn-8 (Trevarrow et al., 1990); 64.86±8.44% (mean±s.d.) of cells within the GCL were *isl2b*:GFP^{+} (Fig. 1A).

To create an ON injury, we performed ON transection (ONT). Injured retinae from the left eye (ONT+) and sham surgery retinae from the right eye (ONT−) were collected at 1, 3, 7 or 14 days post-injury (dpi) (Fig. 1B). We confirmed that there were no differences in cell number between the uninjured left and right eye (left eye: 9844.44±1214.04 cells/mm^2; right eye: 10,118.44±1688.71 cells/mm^2; n=6; P=0.6735, Mann-Whitney test). To quantify RGC survival after ONT, we counted *isl2b*:GFP^{+} RGCs from eight regions (four in the peripheral retina and four in the central retina; Fig. 1B), then divided counts from the ONT+ retina by those from the ONT− retina of the same fish. RGC survival was 94.44±5.45% at 1 dpi and 92.52±3.54% at 3 dpi; however, survival decreased to 76.35±2.58% at 7 dpi (P=0.0009). At 14 dpi, RGC numbers recovered to 98.71±4.82% (Fig. 1C,D).

isl2b:GFP intensity in ONT+ RGCs declined by 40.43±9.99% at 7 dpi relative to ONT− RGCs (P<0.0001), raising the possibility that GFP intensity was falling below the detection threshold after

[1]Eye Center of Xiangya Hospital, Central South University, 410008 Changsha, Hunan, People's Republic of China. [2]Department of Ophthalmology, The University of Pittsburgh School of Medicine, Pittsburgh, PA 15213, USA. [3]Hunan Key Laboratory of Ophthalmology, 410008 Changsha, Hunan, People's Republic of China. [4]Department of Bioengineering, University of Pittsburgh Swanson School of Engineering, Pittsburgh, Pennsylvania, United States of America. [5]Department of Developmental Biology, Louis J. Fox Center for Vision Restoration, The University of Pittsburgh School of Medicine, Pittsburgh, PA 15213, USA.

*Authors for correspondence (kuwajima@pitt.edu; grossjm@pitt.edu)

T.K., 0000-0002-8398-3131; J.M.G., 0000-0002-9422-6312

Handling Editor: Florent Ginhoux
Received 8 April 2021; Accepted 23 August 2021

Development (2022) 149, dev199694. doi:10.1242/dev.199694

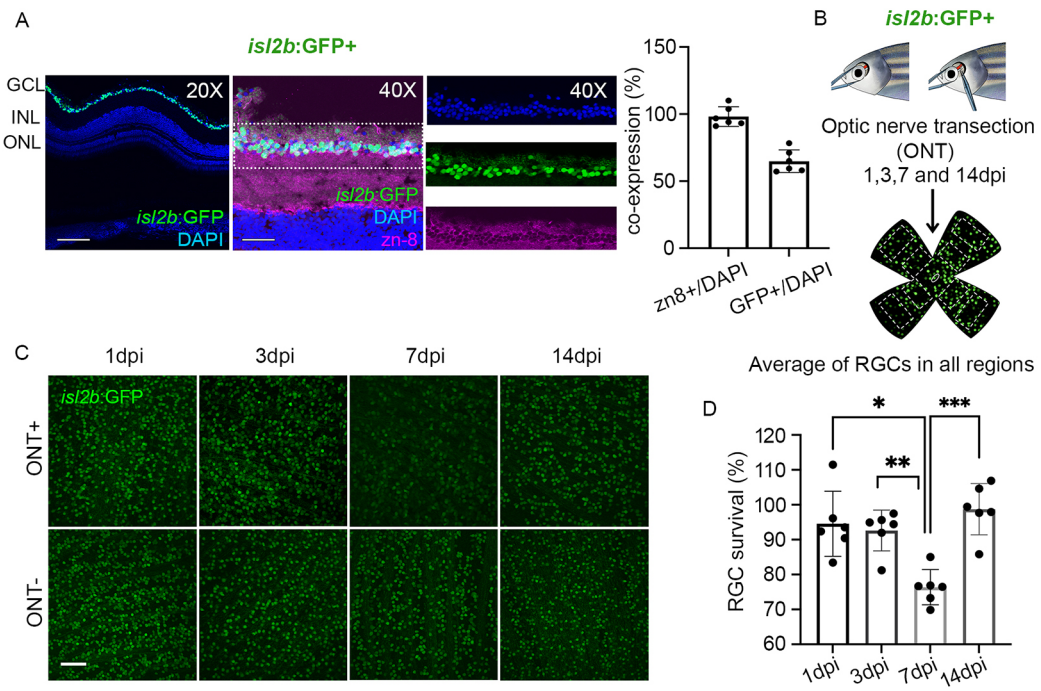

Fig. 1. Zebrafish RGCs are preserved after optic nerve transection. (A) Immunolabeling of RGCs in the GCL with zn-8 (magenta) in the adult *isl2b*:GFP (green) retinae. Shown are a retinal cross section (20×) and high magnification view of the GCL (40×). Quantification revealed that ~65% of DAPI (blue)-stained RGCs were *isl2b*:GFP$^+$ (*n*=xxx). Scale bars: 100 µm (20×); 50 µm (40×). (B) Overview of ONT and RGC survival analyses. (C) Images of flat-mount retinae at 1, 3, 7 and 14 dpi. Scale bar: 50 µm. (D) RGC survival percentages at 1, 3, 7 and 14 dpi (*n*=6/day). Graphs show mean±s.d.; **P*<0.05; ***P*<0.01; ****P*<0.001; Kruskal–Wallis ANOVA with Dunn's multiple comparisons. Data derived from three experiments.

ONT as a result of compromised health rather than death of *isl2b*:GFP$^+$ RGCs. Cleaved caspase-3 immunostaining revealed that 12.44±1.79% (mean±s.e.m.) of RGCs in the ONT+ retinae were cleaved caspase-3$^+$ at 7 dpi, compared with 0.06±0.01% of RGCs in the ONT− retina (Fig. S1). Moreover, no bromodeoxyuridine (BrdU)$^+$ cells were detected in the GCL of ONT+ retinae at 7 dpi, indicating that RGCs had not yet regenerated. Taken together, these data indicate that, despite transient reduction in *isl2b*:GFP levels and limited death, most *isl2b*:GFP$^+$ RGCs are indeed preserved in zebrafish after ONT.

Identification of neuroprotective factors and pathways after ONT

To identify neuroprotective signals/pathways in RGCs, *isl2b*:GFP$^+$ RGCs were isolated by fluorescence-activated cell sorting (FACS) from ONT+ and ONT− retinae at 24 h post-injury (hpi) and analyzed by RNA sequencing (RNA-seq) (Fig. 2A). We identified 308 differentially expressed genes (DEGs) (Fig. 2B), of which 56 were upregulated and 252 were downregulated (Tables S2 and S3). We reasoned that neuroprotective factors would be upregulated upon ONT, and the upregulated DEG group included *stat3*, *irf9*, *sox11b*, *lepr* and *socs3b*, which encode components/regulators of the Jak/Stat signaling pathway (Fig. 2C; Villarino et al., 2017), in addition to other neuroprotective and pro-regenerative genes, such as *gap43* (Chung et al., 2020), *atf3* (Kole et al., 2020) and *atoh7* (Brodie-Kommit et al., 2021). Moreover, the interferon regulatory factor genes *irf9* and *irf1b* (Langevin et al., 2013), and the chemokine receptor *cxcr4b* (García-Cuesta et al., 2019), were also upregulated. Although these genes have been shown to be expressed in rodent RGCs after injury (Dvoriantchikova et al., 2012; Hilla et al., 2021), it is also possible that a small number of macrophages and microglia contaminated our sorted *isl2b*:GFP$^+$ RGCs. Pathway enrichment analyses indicated that Jak/Stat signaling was the most highly enriched pathway in RGCs after ONT (Fig. 2D). Furthermore, DEGs associated with the adipocytokine signaling pathway, which regulates Stat3-mediated signals (Kadye et al., 2020), were also enriched in RGCs after ONT (Fig. 2D). Downregulated DEGs revealed that neuroactive ligand receptor interactions, MAPK, and calcium signaling pathways were all significantly changed after ONT (Fig. 2D).

We also investigated gene expression changes at 12 hpi. The same selection criteria as for 24 hpi analyses yielded limited numbers of DEGs at 12 hpi, with five upregulated and three downregulated (Table S4). Relaxing our selection criteria from a false discovery rate (FDR) *P*-value <0.05 to a *P*-value <0.05 revealed 49 upregulated and 31 downregulated DEGs (Tables S5 and S6). *stat3* and *socs3b* were amongst the upregulated group, further suggesting activation of the Jak/Stat in RGCs after ONT.

Jak/Stat pathway activity is required for RGC survival after ONT

Jak/Stat activity contributes to RGC survival in multiple injury contexts (Boyd et al., 2003; Huang et al., 2007; Luo et al., 2007) and facilitates ON and retinal regeneration (Elsaeidi et al., 2014; Kassen et al., 2009; Leibinger et al., 2013; Mehta et al., 2016; Park et al., 2004; Todd et al., 2016; Zhao et al., 2014). To confirm Jak/Stat pathway activation after ONT, we assessed phosphorylated-Stat3 (pStat3) levels in ONT+ and ONT− retinae (Fig. 3A; Movie 1). pStat3 levels were significantly increased in ONT+ RGCs (Fig. 3B; *P*<0.01), supporting the notion that Stat3 may be neuroprotective after ONT. To determine whether Jak/Stat pathway activity is required for RGC survival after ONT, we performed intravitreal (IV) injections of a pan-Jak inhibitor, Pyridone 6 (P6), or 0.05% DMSO at the time of ONT and again at 1 dpi (Fig. 3C). P6 injection resulted

Development (2022) 149, dev199694. doi:10.1242/dev.199694

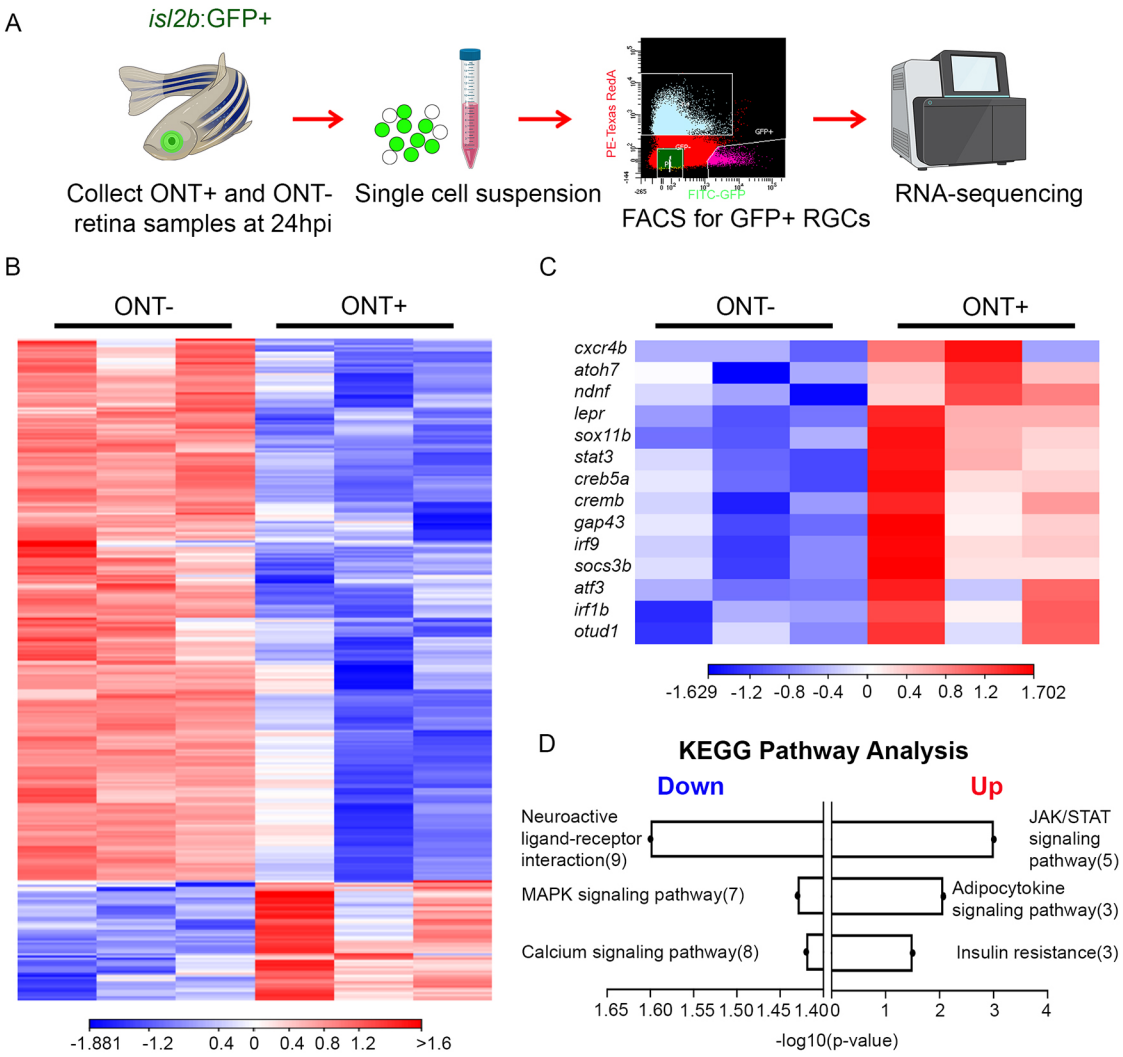

Fig. 2. Identification of DEGs in *isl2b*:GFP$^+$ RGCs after ONT. (A) Experimental workflow for FACS-isolation of *isl2b*:GFP$^+$ RGCs. An example FACS plot showing a cell-sorting gate is included. Icons were adapted from BioRender.com. Number of experiments=1. (B) Heatmap showing hierarchical clustering of 308 DEGs at 24 hpi from three biological replicates. (C) Heatmap highlighting DEGs of interest based on known neuroprotective and pro-regenerative functions. Heatmap legends show log$_2$TPM. (D) Pathway enrichment analysis using the KEGG database showing top-3 down- and upregulated pathways after ONT.

in significant reductions to pStat3 levels in ONT+ RGCs at 1 dpi and 7 dpi, supporting the efficacy of P6 in blocking Jak activation in zebrafish (Fig. 3D,E). We next quantified *isl2b*:GFP$^+$ RGC survival at 7 dpi when Jak activity was impaired (Fig. 3F,G). DMSO had no effect on RGC survival, and neither did P6 alone (P=0.4796; Fig. 3G). However, IV P6 injection in conjunction with ONT resulted in a significant reduction in RGC survival to 39.44±6.99% (P<0.0001) and a corresponding increase in cleaved caspase-3 levels in ONT+ RGCs (Fig. S3). These data demonstrate a role for Jak/Stat pathway activity in protecting zebrafish RGCs after ONT.

Innate immune response involvement after ONT

After ONI, the effects of injury-activated immune responses are varied. In some contexts, immune responses stimulate the recruitment and activation of leukocytes, which generate secondary signals to modulate RGC survival and death pathways (Bariş and Tezel, 2019; Mac Nair et al., 2016; Nadal-Nicolás et al., 2017; Williams et al., 2017), whereas in others the stimulation of limited neuroinflammation induces pro-survival and regenerative responses (Kanagaraj et al., 2020; Todd et al., 2019). In zebrafish, leukocyte activity accelerates axonal regeneration after neuronal damage (Tsarouchas et al., 2018), including in RGCs after ON crush (Van Dyck et al., 2021). With this in mind, we next investigated how components of the innate immune system respond to ONT in zebrafish and whether they contribute to RGC vulnerability. We focused on macrophages/microglia, leukocytes that accumulate in the zebrafish retina after a variety of injury types and facilitate repair and regeneration (Leach et al., 2021; White et al., 2017). In zebrafish, the 4C4 antibody recognizes an unidentified protein expressed by macrophages/microglia (Craig et al., 2008). Consistent with other reports (Mitchell et al., 2018), 4C4$^+$ macrophages/microglia were located throughout the ONT− retina, including in the GCL (Fig. 4A,B; Movie 2). At 1 dpi, the number of 4C4$^+$ cells appeared to increase in the GCL (Fig. 4A,B). Similarly, utilizing *mpeg1*:mCherry transgenic fish (Ellett et al., 2011), we observed an apparent increase in mCherry$^+$ macrophages/microglia in the ONT+ GCL at 1 dpi (Fig. 4C). Owing to the morphology and close proximity of macrophages/microglia in the ONT retinae, it was difficult to identify single

Development (2022) 149, dev199694. doi:10.1242/dev.199694

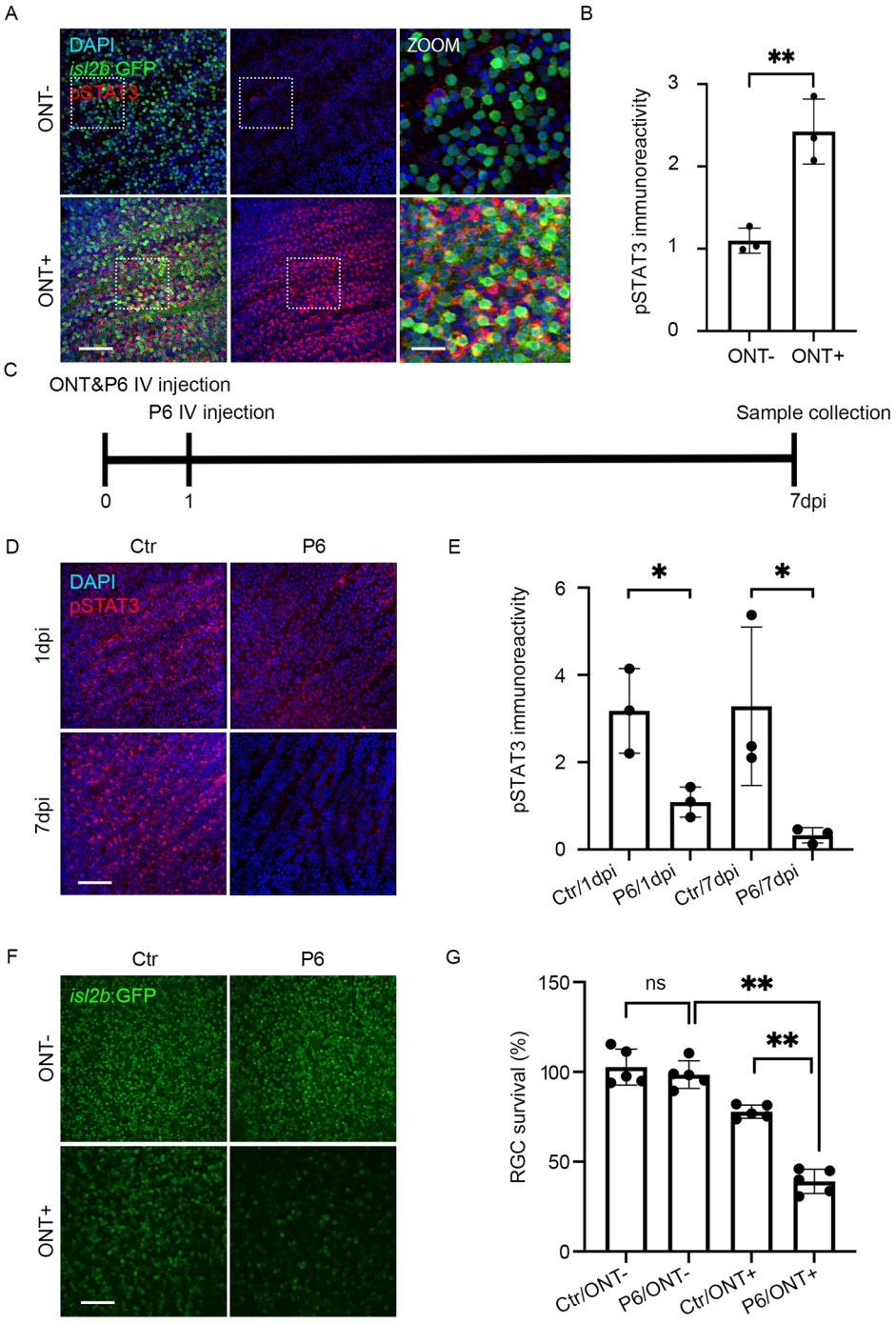

Fig. 3. Jak/Stat pathway activity is required for RGC survival after ONT. (A) pStat3 expression (red) in flat-mount *isl2b*:GFP ONT– and ONT+ retinae at 1 dpi. Nuclei are stained with DAPI (blue). Right-hand panels show 3× magnifications of the boxed regions in the 40× images. (B) Quantification of pStat3 levels at 1 dpi. pStat3 levels in ONT+ RGCs are shown relative to those in ONT– retinae. Shown are mean±s.d. of n=3 for each group; $^{**}P$<0.01; Mann–Whitney test. Data derived from three experiments. (C) Experimental protocol to assess Jak requirement for RGC survival after ONT. (D) pStat3 expression in ONT+ *isl2b*:GFP retinal flat mounts at 1 and 7 dpi with or without IV injection of the Jak inhibitor P6. DMSO was used as control (Ctr). (E) Quantification of pStat3 expression after P6 application at 1 and 7 dpi. n=3/condition. Shown are mean±s.d.; $^{*}P$<0.05, Mann–Whitney test. Data derived from three experiments. (F) Images of P6- or DMSO-injected flat-mount *isl2b*:GFP retinae at 7 dpi. (G) Quantification of RGC survival after P6 injection (n=5/condition). Shown are mean±s.d.; $^{**}P$<0.01; Kruskal–Wallis ANOVA with Dunn's multiple comparisons. Scale bars: 50 µm (A, main panels; D,F); 150 µm (A, zoom). Data derived from four experiments.

macrophages/microglia for counting and therefore we quantified the percentage area covered by mCherry$^+$ cells within the GCL (Fig. 4D). Compared with ONT– retinae, mCherry$^+$ cells covered nearly six times more GCL area after ONT (P=0.0006; Fig. 4D). Macrophage/microglia morphologies change upon activation, whereby quiescent cells with a ramified morphology take on a more spherical/amoeboid shape when activated (Karlstetter et al., 2015; Mitchell et al., 2018). Morphological differences were evident in both 4C4$^+$ and mCherry$^+$ cells within the GCL of ONT+ retinae (Fig. 4B,C), and quantification of mCherry$^+$ cell sphericity revealed a significant increase at 1 dpi (Fig. 4E; P<0.0001); collectively, these data show that macrophages/microglia accumulate in the GCL and become activated after ONT.

Blocking inflammation or depletion of macrophages/microglia protects RGCs after ONT

To test the hypothesis that macrophage/microglia-mediated inflammation might contribute to RGC death after ONT, we inhibited inflammation after ONT by dexamethasone treatment, a strategy shown to protect RGCs in other injury models (Bollaerts et al., 2019; Dutt et al., 2010; Gallina et al., 2015; Jovanovic et al., 2020), and quantified RGC survival. Experimentally, 2 µl of 10 µM dexamethasone or 0.05% DMSO (vehicle control) was IV injected into *isl2b*:GFP fish at the time of ONT and again at 1 dpi and tissue was collected at 7 dpi (Bollaerts et al., 2019) (Fig. 3C). Dexamethasone efficacy was verified via qRT-PCR for *pxr* (also known as nr1i2), a dexamethasone-regulated gene (Fig. S4A;

Development (2022) 149, dev199694. doi:10.1242/dev.199694

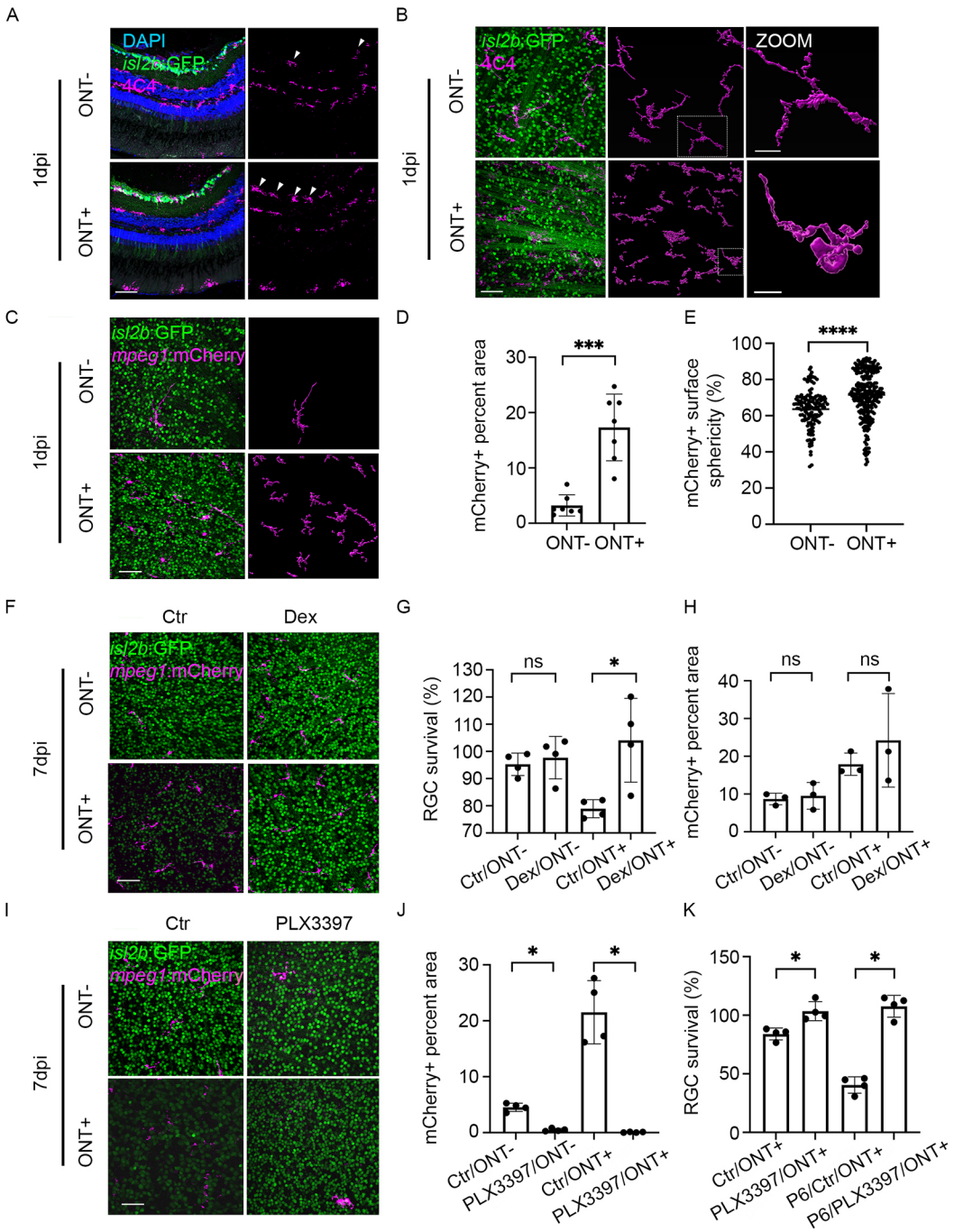

Fig. 4. Macrophages/microglia are recruited to the GCL after ONT and mediate RGC death. (A,B) Immunostaining of 4C4 (magenta) on *isl2b*:GFP retinal cryosections (A) and retinal flat mounts at 1 dpi with surface renderings of 4C4$^+$ macrophages/microglia generated in Imaris (B). (C) Images of retinal flat-mounts from *isl2b*:GFP;*mpeg1*:mCherry animals at 1 dpi. mCherry+ macrophages/microglia (magenta) surfaces were rendered in Imaris. (D) Quantification of the surface area within the GCL occupied by mCherry$^+$ macrophages/microglia at 1 dpi (n=7/condition). Shown are mean±s.d.; ***P<0.001; Mann–Whitney test. Data derived from one experiment. (E) Violin plot showing a significant increase in sphericity of mCherry+ macrophages/microglia in ONT+ retinae compared with ONT− controls (n=140 in ONT− and n=272 in ONT+). ****P<0.0001; unpaired t-test with Welch's correction. (F) Flat-mount images of *isl2b*:GFP;*mpeg1*:mCherry retinae after IV injection of dexamethasone (Dex) or DMSO (Ctr) at 7 dpi. (G) RGC survival in dexamethasone-treated retinae increased significantly at 7 dpi compared with control (n=4/condition). Shown are mean±s.d.; *P<0.05; Kruskal–Wallis ANOVA test with Dunn's multiple comparisons. Data derived from three experiments. (H) Quantification of mCherry$^+$ macrophage/microglia coverage of the GCL after ONT and dexamethasone or DMSO injection (n=3/condition). Shown are mean±s.d.; Kruskal–Wallis ANOVA test with Dunn's multiple comparisons. No significant differences were detected. Data derived from three experiments. (I) Flat-mount images of *isl2b*:GFP;*mpeg1*:mCherry retinae after PLX3397 treatment or housed in system water (Ctr) at 7 dpi. (J) Quantification of mCherry$^+$ macrophage/microglia coverage of the GCL after ONT and PLX3397 treatment (n=4/condition). Shown are mean±s.d.; *P<0.05; Kruskal–Wallis ANOVA test with Dunn's multiple comparisons. Data derived from three experiments. (K) RGC survival in PLX3397-treated retinae increased significantly at 7 dpi compared with control. Similarly, RGC survival in PLX3397-treated retinae increased significantly after P6 addition compared with DMSO controls (n=4/condition). Shown are mean±s.d.; *P<0.05; Mann–Whitney test. Data derived from three experiments. Scale bars: 50 µm. ns, not significant.

Development (2022) 149, dev199694. doi:10.1242/dev.199694

Shi et al., 2010). Dexamethasone alone had no effect on *isl2b*:GFP$^+$ RGC survival in the ONT− retina (96.56±8.67%, P=0.5998), but significantly increased survival of ONT+ RGCs at 7 dpi, compared with DMSO controls (104.1±13.35%, P<0.05; Fig. 4G). Dexamethasone prevents the recruitment of macrophages/microglia in some contexts (Tsarouchas et al., 2018; White et al., 2017), but not others (Chatzopoulou et al., 2016; Warchol, 1999; Xie et al., 2019; Leach et al., 2021). Quantification of the percentage of the GCL covered by *mpeg1*:mCherry$^+$ macrophages/microglia in DMSO- and dexamethasone-injected retinae revealed no significant differences after ONT (Fig. 4H; P=0.0623). Quantification of mCherry$^+$ cell sphericity, as a proxy for macrophage/microglia activity, revealed no significant differences between dexamethasone-treated retinae and controls at 7 dpi (Fig. S4B). However, dexamethasone suppressed the expression of inflammatory markers, such as *il1b* (Mitchell et al., 2019; Tsarouchas et al., 2018), *il6* and *tnfa* (Bessler et al., 1999), after ONT (Fig. S4A).

Previous reports have identified roles for microglia in contributing to RGC death after a variety of insults (Bosco et al., 2008; Jovanovic et al., 2020; Takeda et al., 2018). However, other studies have shown that microglia are dispensable for RGC survival after ON crush (Hilla et al., 2017), and may instead provide neuroprotective and/or pro-regenerative signals (Bell et al., 2018; Sappington et al., 2006). To test directly the requirement of macrophages/microglia in modulating RGC death in zebrafish after ONT, we depleted macrophages/microglia using PLX3397, a potent inhibitor of the colony–stimulating factor 1 receptor (Csf1r). Csf1r activity is required for macrophage/microglia differentiation (Lin et al., 2008; Sherr et al., 1985) and PLX3397 has been utilized effectively in zebrafish (e.g. Conedera et al., 2019; Leach et al., 2021; Van Dyck et al., 2021). Animals were immersed in 500 nM PLX3397 1 day prior to ONT and retinae were collected at 7 dpi. To validate the efficiency of macrophage/microglia depletion by PLX3397, we quantified the percentage area of the GCL occupied by *mpeg1*:mCherry$^+$ macrophages/microglia. PLX3397 significantly reduced the coverage of *mpeg1*:mCherry$^+$ cells in both the ONT− and ONT+ GCL (Fig. 4I,J). Similar to dexamethasone-mediated RGC protection (Fig. 4F,G), PLX3397-mediated depletion of macrophages/microglia significantly increased RGC survival at 7 dpi (103.49±12.01%, P<0.05; Fig. 4I,K) concomitant with decreased cleaved caspase-3 levels in ONT+ RGCs (Fig. S3). PLX3397-mediated depletion of macrophages/microglia also rescued RGC survival and decreased cleaved caspase-3 levels at 7 dpi after Jak/Stat pathway inhibition using P6 (107.60±9.32%, P<0.05; Fig. 4K; Figs S2 and S3), indicating that Jak/Stat activity is dispensable in the absence of macrophage/microglia recruitment. pStat3 was detected in both RGCs and also some *mpeg1*:mCherry$^+$ macrophages/microglia in ONT+ retinae (Fig. S5A). Expression of pStat3 was eliminated in both cell types in the P6/PLX3397-treated ONT+ retinae (Fig. S5B). However, the observation that pStat3 was detected in both RGCs and macrophages/microglia after ONI indicates that the effects of Jak/Stat pathway inhibition could reflect activities in one or both cell types. Future studies targeting loss- and/or gain-of-function assays to RGCs and/or leukocytes will be needed to parse contributions from each cell type to RGC survival after ONI.

Collectively, these data support a model in which crosstalk between macrophages/microglia and RGCs, mediated by Jak/Stat pathway activity, regulates RGC survival after ONI. As noted above, Stat3 upregulation has been associated with RGC survival in some experimental contexts (Huang et al., 2007; Luo et al., 2007). Despite this, overall RGC survival is limited under physiological conditions, with over 90% of RGCs lost within 28 days after injury in mice (Li et al., 2020). This is not true for all mammals, however. Indeed, the naked mole-rat retains many RGCs after injury, to at least 28 days (Park et al., 2017). Interestingly, although pStat3 is nearly absent in mouse RGCs, even after injury, it increases significantly in mole-rat RGCs after ON crush, supporting a possible role for Stat3 activity in RGC neuroprotection.

Counter to our expectations, pStat3 localization was predominantly cytoplasmic in ONT+ RGCs, rather than nuclear (Fig. 3A; Movie 1). This observation is consistent with cytoplasmic pStat3 localization in the regenerating zebrafish retina (Elsaeidi et al., 2014) and in mouse motor neurons responding to cytokine stimulation (Selvaraj et al., 2012). Stat3 possesses transcription-independent functions such as cytoplasmic regulation of autophagy (Shen et al., 2012). Stat3 also localizes to mitochondria after cytokine stimulation in mouse RGCs where it regulates metabolic functions and enhances axon regeneration after ONI (Luo et al., 2016). Thus, it is possible that the function of Stat3 in RGC neuroprotection could be independent of transcription.

Not all zebrafish RGCs survive ONT and cleaved caspase-3$^+$ RGCs appeared to be distributed in a non-random pattern in the ONT+ retina (Fig. S1). This may indicate that there are RGC subtype(s) that are more susceptible to ONI, similar to observations in mice (Tran et al., 2019). RGC subtypes in zebrafish have been recently characterized (Kölsch et al., 2021) and additional studies will be required to determine whether specific subtypes are lost after ONT, and, if so, whether these subtypes lack the ability to upregulate Jak/Stat activity after injury. Finally, it will be of interest to identify the signals emanating from macrophages/microglia that activate death and/or pro-survival pathways in zebrafish RGCs after injury, as these would also be promising targets around which neuroprotective therapies for glaucoma could be developed (García-Bermúdez et al., 2021; Rashid et al., 2019).

MATERIALS AND METHODS

Animals

Zebrafish (*Danio rerio*) in this study were 3-5 months old and an equal number of males and females were used in all experiments. Transgenic lines used were *isl2b*:GFP (Pittman et al., 2008) and *mpeg1*:mCherry (Ellett et al., 2011; a gift from Dr Neil Hukriede, University of Pittsburgh, USA). Animals were maintained under standard conditions at 28.5°C on a 14 h light/10 h dark cycle. There were no differences in outcomes based on sex of the fish and therefore all data were combined for analyses. All animals were treated in accordance with provisions established by the University of Pittsburgh School of Medicine Institutional Animal Care and Use Committee. Biological replicates are stated in figure legends for each experiment. At least three independent biological replicates were used per experiment.

ONT

ONT was performed as previously described (Elsaeidi et al., 2014; Zou et al., 2013). Zebrafish were anesthetized in 0.03% tricaine buffer (MS-222; Fisher Scientific) and placed on a moist tissue paper under a dissecting scope (Leica E65S). ONT surgery was performed on the left eye. After removal of the connective tissue, the eyeball was pulled out from the orbit gently using forceps. The ON and ophthalmic artery, which runs along with the ON, were exposed and the ON was then completely transected using additional forceps, after which the eye was placed back in the orbit. Any animals in which bleeding was observed were euthanized and not used for analysis. The right eye was subjected to a sham surgery as control: connective tissue was removed, the eye was pulled out from the orbit gently, and then placed back in the orbit. Fish were returned to system water in separate tanks to recover.

Development (2022) 149, dev199694. doi:10.1242/dev.199694

RGC isolation and FACS

Retinae were harvested from *isl2b*:GFP zebrafish at 12 and 24 h post-injury (hpi) in biological triplicate. Four retinae were collected per sample. For retinal isolations and cell dissociation, animals were euthanized by tricaine overdose and transferred to PBS for enucleation. To achieve a single-cell suspension, the eyeball was rinsed in 1× PBS post-enucleation and incubated in StemPro Accutaset Cell Dissociation Reagent (Thermo Fisher, #A1110501) at 28.5°C for 40 min in a water bath. The cell suspension was then passed through a 70-µm cell strainer (Fisher Scientific) and gently pelleted by centrifugation at 2189 rpm (450 ***g***) for 5 min at 4°C. After two washes in ice-cold 1× PBS, cells were resuspended in ice cold 5% fetal bovine serum in 1× PBS. GFP^+ cells were sorted using a FACS Aria IIu cell sorter (BD Biosciences) at the Flow Cytometry Core at the University of Pittsburgh School of Medicine Department of Pediatrics. The gate for FACS was set by GFP intensity for wild-type (non-transgenic) and both injured (ONT) and intact (control) *isl2b*:GFP samples. The same gating settings were used for both the ONT and control RGC samples and for all biological replicates.

RNA-seq and bioinformatics analyses

Library preparation, quality control analysis, and next-generation sequencing were performed by the Health Sciences Sequencing Core at Children's Hospital of Pittsburgh as previously described (Leach et al., 2021). cDNA sequencing libraries were prepared using a SmartSeq HT kit (Takara Bio) and Illumina Nextera XT kit (Illumina Inc.) and 2×75 paired-end, 150 cycle sequencing was performed on a NextSeq 500 system (Illumina), aiming for 40 million reads per sample. After sequencing, raw read data were imported to the CLC Genomics Workbench (Qiagen Digital Insights) licensed through the Molecular Biology Information Service of the Health Sciences Library System at the University of Pittsburgh. After mapping trimmed reads to the *Danio rerio* reference genome (assembly GRCz11), DEGs from the 24 hpi time point were identified using the following filter: the maximum of the average group RPKM value >1.5, absolute fold change >2, FDR *P*-value <0.05. Genes with TPM=0 in one or more replicates were excluded. This filtering strategy was also used for DEGs at 12 hpi and a second analysis was performed in which the FDR *P*-value <0.05 was switched to a *P*-value <0.05. Pathway enrichment analyses were performed using DAVID Bioinformatics Resources 6.8 (https://david.ncifcrf.gov) and using the KEGG database.

Pharmacological experiments

To assess toxicity and efficacy, the JAK inhibitor Pyridone 6 (P6), or dexamethasone (both Sigma-Aldrich) were IV injected into the intact and injured retina at several different concentrations, as previously described (Elsaeidi et al., 2014), and RGC survival was quantified. Similar to previous studies (Bollaerts et al., 2019; Elsaeidi et al., 2014), 5 µM P6 and 10 µM dexamethasone were utilized. The first dose of each compound (2 µl) was injected immediately after ONT (0 dpi) and the second dose (2 µl) was injected at 1 dpi. For all control doses, 2 µl of 0.05% DMSO was injected. To deplete macrophages/microglia, fish were immersed in 500 nM PLX3397 (Fisher Scientific) or 0.05% DMSO (control) in system water, as previously described (Kanagaraj et al., 2020). PLX3397 exposure started 1 day before ONT and system water containing PLX3397 was replaced daily during the experiment.

Immunohistochemistry

Immunofluorescence staining on retinal cryosections and flat-mounted retinae were performed as previously described (Uribe and Gross, 2007; Zou et al., 2013) with the addition of an antigen-retrieval step consisting of 100% methanol incubation at −20°C for 30 min for staining pStat3 (MBL International Corporation, D128-3) and cleaved caspase-3 (Abcam, ab13847). For retinal flat-mounts, after euthanasia, fish were decapitated and heads were fixed in 4% paraformaldehyde (PFA) at 4°C overnight. The retina was dissected in ice-cold PBS, washed in PBST (0.1% Triton X-100 in PBS), and then incubated in a 1.5 ml tube on a rotator overnight at 4°C with antibodies against 4C4 (1:200, a kind gift of Dr Peter Hitchcock, University of Michigan School of Medicine, USA; Craig et al., 2008), pStat3 (1:100, MBL International Corporation), cleaved caspase-3 (1:200, Abcam) and mCherry (1:200, Takara Bio/Clontech Laboratories, 632543). Retinae were then washed in PBST for 3×10 min at room temperature and incubated with goat-anti mouse Cy3 (1:250, Jackson ImmunoResearch Laboratories, 115-165-166) or goat-anti rabbit Alexa 647 (1:500, Cell Signaling Technology, 8940) secondary antibodies for 3 h at room temperature. Samples were then washed with PBST for 3×10 min and carefully cut into four quadrants and mounted on slides with DAPI VECTASHIELD (Vector Laboratories, H-1200). For cryosections, samples were prepared as previously described (Uribe and Gross, 2007); zn-8 (Zebrafish International Resource Center) was used at 1:200 and all other antibodies were used at the same concentrations as for the retinal flat-mount.

BrdU incorporation assays

Adult *isl2b*:GFP+ fish were immersed in 10 mM BrdU (Sigma-Aldrich) dissolved in system water from 6 dpi to 7 dpi, and sacrificed at 7 dpi. As a positive control for BrdU incorporation and immunohistochemistry, a needle poke injury was performed following previously published protocols (Fausett and Goldman, 2006) and fish were exposed to BrdU for 24 h prior to being sacrificed. Immunohistochemistry for BrdU proceeded as described above for other antibodies, with the addition of a 10-min incubation of 4 N HCl at 37°C to relax chromatin. Anti-BrdU (Abcam, ab6326) was used at 1:200.

Confocal microscopy, image processing and quantification

For *isl2b*:GFP imaging, retinal flat-mounts were prepared as above, with the head fixed in 4% PFA overnight at 4°C and the retina dissected and mounted on the second day. Images were taken using Olympus Fluoview FV1200 laser scanning microscope and a 40× objective (Olympus Corporation). Images were taken from each of the four quadrants (one peripheral and one central per quadrant). Quantification of RGC numbers was performed using particle analysis in ImageJ after setting up a consistent threshold for all images. RGC survival was calculated as the ratio of *isl2b*:GFP^+ RGCs in the left (ONT+ and/or drug treatment) eye/*isl2b*:GFP+ RGCs in the right (ONT− and/or DMSO control) eye of the same fish.

Quantification of macrophages/microglia was performed using Imaris 9.6.0 (Bitplane). Confocal images were first converted into Imaris files, and 3D-rendered surfaces were then created for mCherry or 4C4 using the same algorithm (smoothing=0.4 µm, absolute intensity threshold=1560, objects area>50 μm^2) for each dataset. Quantification of total surface area and sphericity was performed using Imaris. Measurements were exported and statistically assessed using Prism 9.0 (GraphPad).

For GFP fluorescence intensity quantification, the GFP signal intensity of 30 randomly selected RGCs in the ONT+ and ONT− retina per fish (n=6) was measured using Fiji ImageJ and the corrected total cell fluorescence (CTCF) was obtained following the protocol of L. Hammond (The University of Queensland, Australia; https://theolb.readthedocs.io/en/latest/imaging/measuring-cell-fluorescence-using-imagej.html). Briefly, using the freehand tool in ImageJ, single RGCs were outlined as a region of interest and GFP intensity was measured as well as the background fluorescence for every retina. CTCF was then calculated as follows: integrated density−(area of selected cell×mean fluorescence of background readings). Relative intensity was calculated as the ratio of the CTCF in ONT+ RGCs divided by that of ONT− RGCs.

Localization of pStat3 expression to RGCs was confirmed with surface creation in Imaris 9.6.0. Quantification of pStat3 levels was performed as described (Osborne et al., 2018) using Fiji (ImageJ). Briefly, *isl2b*:GFP labeling was used to identify the location and depth of the GCL. RGC volumes were converted to *z*-projections and background subtraction and speckle removal was performed on all images. Threshold levels for pStat3 were determined from ONT− samples and consistent thresholds were then applied to all images in ONT+ samples and integrated density was measured. The expression level of pStat3 was calculated as the ratio of the average integrated density of pStat3 in 1 dpi, 7 dpi, P6/1 dpi or P6/7 dpi retinae to the average integrated density of the contralateral ONT− eye.

Cleaved caspase-3 levels were quantified in two ways: (1) the number of cleaved caspase-3+ nuclei relative to the number of RGCs or (2) the ratio of

Development (2022) 149, dev199694. doi:10.1242/dev.199694

thresholded area pixels of staining to the number of DAPI+ nuclei. For the latter, cleaved caspase-3 staining volumes were converted to *z*-projections with a consistent number of *z*-sections between samples. Background subtraction and speckle removal was performed on all images using Fiji (ImageJ). Threshold levels were determined from control/ONT+ samples and applied consistently for all images. Pixels of cleaved caspase-3 staining areas were then measured and recorded. DAPI+ nuclei counts were performed as described for RGC quantification.

Quantitative real-time PCR (qRT-PCR)

RNA was extracted from adult *isl2b*:GFP+ retinae using Trizol reagent (Fisher Scientific, 15-596-018) and cDNA generated using the iScript cDNA Synthesis Kit (Bio-Rad Laboratories). For each treatment group, three biological replicates were collected with each replicate consisting of three retinae from three different fish. qRT-PCR was performed on a CFX384 Touch Real-Time PCR Detection System (Bio-Rad Laboratories) using the iTaq Universal SYBR Green Supermix (Bio-Rad Laboratories). Primer sequences are provided in Table S1. Gene expression fold change was calculated using the comparative CT method ($2-\Delta\Delta CT$) and expression in DMSO/ONT− retinae was normalized to 1 as the control (Livak and Schmittgen, 2001). *gapdh* was used as the housekeeping gene in these experiments (Barber et al., 2005).

Statistics

All statistical analyses were performed using Prism 9.0 (GraphPad). Data are presented as mean±s.d., with the exception of cleaved caspase-3 images, which show mean±s.e.m. For multiple comparisons, Kruskal–Wallis ANOVA followed by Dunn's multiple comparisons tests between groups were performed. For comparisons between two groups, non-parametric Mann–Whitney tests were performed, with the exception of sphericity comparison, for which an unpaired *t*-test with Welch's correction was performed. *P*-values, sample sizes and statistical analyses for each experiment are included in the figure legends.

Acknowledgements

We are grateful to Dick Barrett and Ben Carr for technical assistance and to Dr Hugh Hammer for expert zebrafish husbandry.

Competing interests

The authors declare no competing or financial interests.

Author contributions

Conceptualization: T.K., J.M.G.; Methodology: K.L.L., T.K.; Formal analysis: S.C.; Investigation: S.C.; Writing - original draft: S.C.; Writing - review & editing: J.M.G.; Supervision: T.K., J.M.G.; Project administration: J.M.G.; Funding acquisition: J.M.G.

Funding

This work was supported by a grant from the BrightFocus Foundation National Glaucoma Research Program (G2020277 to J.M.G.); an unrestricted grant from Xiangya Hospital, Central South University and China Scholarship Council for studying in Pittsburgh (to S.C.); a National Eye Institute Core Grant (P30-EY08098) to the Department of Ophthalmology; the Eye and Ear Foundation of Pittsburgh, and an unrestricted grant from Research to Prevent Blindness. Deposited in PMC for release after 12 months.

Data availability

Raw read and processed RNA-seq data have been deposited in Gene Expression Omnibus under accession number GSE171426.

Peer review history

The peer review history is available online at https://journals.biologists.com/dev/article-lookup/doi/10.1242/dev.199694.

References

Almasieh, M., Wilson, A. M., Morquette, B., Cueva Vargas, J. L. and Di Polo, A. (2012). The molecular basis of retinal ganglion cell death in glaucoma. *Prog. Retin. Eye Res.* **31**, 152-181. doi:10.1016/j.preteyeres.2011.11.002

Barber, R. D., Harmer, D. W., Coleman, R. A. and Clark, B. J. (2005). GAPDH as a housekeeping gene: analysis of GAPDH mRNA expression in a panel of 72 human tissues. *Physiol. Genomics* **21**, 389-395. doi:10.1152/physiolgenomics.00025.2005

Bariş, M. and Tezel, G. (2019). Immunomodulation as a neuroprotective strategy for glaucoma treatment. *Curr Ophthalmol Rep* **7**, 160-169. doi:10.1007/s40135-019-00212-1

Bell, K., Und Hohenstein-Blaul, N. v. T., Teister, J. and Grus, F. (2018). Modulation of the immune system for the treatment of glaucoma. *Curr. Neuropharmacol.* **16**, 942-958. doi:10.2174/1570159X15666170720094529

Bessler, H., Mendel, C., Straussberg, R., Gurary, N., Aloni, D. and Sirota, L. (1999). Effects of dexamethasone on IL-1β, IL-6, and TNF-α production by mononuclear cells of newborns and adults. *Neonatology* **75**, 225-233. doi:10.1159/000014099

Bollaerts, I., Van Houcke, J., Beckers, A., Lemmens, K., Vanhunsel, S., De Groef, L. and Moons, L. (2019). Prior exposure to immunosuppressors sensitizes retinal microglia and accelerates optic nerve regeneration in Zebrafish. *Mediators Inflamm.* **2019**, 6135795. doi:10.1155/2019/6135795

Bosco, A., Inman, D. M., Steele, M. R., Wu, G., Soto, I., Marsh-Armstrong, N., Hubbard, W. C., Calkins, D. J., Horner, P. J. and Vetter, M. L. (2008). Reduced retina microglial activation and improved optic nerve integrity with minocycline treatment in the DBA/2J mouse model of glaucoma. *Invest. Ophthalmol. Vis. Sci.* **49**, 1437-1446. doi:10.1167/iovs.07-1337

Boyd, Z. S., Kriatchko, A., Yang, J., Agarwal, N., Wax, M. B. and Patil, R. V. (2003). Interleukin-10 receptor signaling through STAT-3 regulates the apoptosis of retinal ganglion cells in response to stress. *Investig. Opthalmol. Vis. Sci.* **44**, 5206-5211. doi:10.1167/iovs.03-0534

Brodie-Kommit, J., Clark, B. S., Shi, Q., Shiau, F., Kim, D. W., Langel, J., Sheely, C., Ruzycki, P. A., Fries, M., Javed, A. et al. (2021). Atoh7-independent specification of retinal ganglion cell identity. *Sci. Adv.* **7**, eabe4983. doi:10.1126/sciadv.abe4983

Chang, E. E. and Goldberg, J. L. (2012). Glaucoma 2.0: neuroprotection, neuroregeneration, neuroenhancement. *Ophthalmology* **119**, 979-986. doi:10.1016/j.ophtha.2011.11.003

Chatzopoulou, A., Heijmans, J. P. M., Burgerhout, E., Oskam, N., Spaink, H. P., Meijer, A. H. and Schaaf, M. J. M. (2016). Glucocorticoid-induced attenuation of the inflammatory response in Zebrafish. *Endocrinology* **157**, 2772-2784. doi:10.1210/en.2015-2050

Chung, D., Shum, A. and Caraveo, G. (2020). GAP-43 and BASP1 in axon regeneration: implications for the treatment of neurodegenerative diseases. *Front. Cell Dev. Biol.* **8**, 567537. doi:10.3389/fcell.2020.567537

Cigliola, V., Becker, C. J. and Poss, K. D. (2020). Building bridges, not walls: spinal cord regeneration in zebrafish. *Dis. Model. Mech.* **13**, dmm044131. doi:10.1242/dmm.044131

Conedera, F. M., Pousa, A. M. Q., Mercader, N., Tschopp, M. and Enzmann, V. (2019). Retinal microglia signaling affects Müller cell behavior in the zebrafish following laser injury induction. *Glia* **67**, 1150-1166. doi:10.1002/glia.23601

Craig, S. E. L., Calinescu, A.-A. and Hitchcock, P. F. (2008). Identification of the molecular signatures integral to regenerating photoreceptors in the retina of the zebra fish. *J. Ocul. Biol. Dis. Infor.* **1**, 73-84. doi:10.1007/s12177-008-9011-5

Diekmann, H., Kalbhen, P. and Fischer, D. (2015). Characterization of optic nerve regeneration using transgenic zebrafish. *Front. Cell. Neurosci.* **9**, 118. doi:10.3389/fncel.2015.00118

Dutt, M., Tabuena, P., Ventura, E., Rostami, A. and Shindler, K. S. (2010). Timing of corticosteroid therapy is critical to prevent retinal ganglion cell loss in experimental optic neuritis. *Invest. Ophthalmol. Vis. Sci.* **51**, 1439-1445. doi:10.1167/iovs.09-4009

Dvoriantchikova, G., Ivanov, D., Barakat, D., Grinberg, A., Wen, R., Slepak, V. Z. and Shestopalov, V. I. (2012). Genetic ablation of Pannexin1 protects retinal neurons from ischemic injury. *PLoS ONE* **7**, e31991. doi:10.1371/journal.pone.0031991

Ellett, F., Pase, L., Hayman, J. W., Andrianopoulos, A. and Lieschke, G. J. (2011). mpeg1 promoter transgenes direct macrophage-lineage expression in zebrafish. *Blood* **117**, e49-e56. doi:10.1182/blood-2010-10-314120

Elsaeidi, F., Bemben, M. A., Zhao, X.-F. and Goldman, D. (2014). Jak/Stat signaling stimulates zebrafish optic nerve regeneration and overcomes the inhibitory actions of Socs3 and Sfpq. *J. Neurosci.* **34**, 2632-2644. doi:10.1523/JNEUROSCI.3898-13.2014

Fausett, B. V. and Goldman, D. (2006). A role for α1 tubulin-expressing Müller glia in regeneration of the injured zebrafish retina. *J. Neurosci.* **26**, 6303-6313. doi:10.1523/JNEUROSCI.0332-06.2006

Gallina, D., Zelinka, C. P., Cebulla, C. M. and Fischer, A. J. (2015). Activation of glucocorticoid receptors in Müller glia is protective to retinal neurons and suppresses microglial reactivity. *Exp. Neurol.* **273**, 114-125. doi:10.1016/j.expneurol.2015.08.007

García-Bermúdez, M. Y., Freude, K. K., Mouhammad, Z. A., van Wijngaarden, P., Martin, K. K. and Kolko, M. (2021). Glial cells in glaucoma: friends, foes, and potential therapeutic targets. *Front. Neurol.* **12**, 169. doi:10.3389/fneur.2021.624983

García-Cuesta, E. M., Santiago, C. A., Vallejo-Díaz, J., Juarranz, Y., Rodríguez-Frade, J. M. and Mellado, M. (2019). The role of the CXCL12/CXCR4/ACKR3 axis in autoimmune diseases. *Front. Endocrinol.* **10**, 585. doi:10.3389/fendo.2019.00585

Hilla, A. M., Diekmann, H. and Fischer, D. (2017). Microglia are irrelevant for neuronal degeneration and axon regeneration after acute injury. *J. Neurosci.* **37**, 6113-6124. doi:10.1523/JNEUROSCI.0584-17.2017

Hilla, A. M., Baehr, A., Leibinger, M., Andreadaki, A. and Fischer, D. (2021). CXCR4/CXCL12-mediated entrapment of axons at the injury site compromises optic nerve regeneration. *Proc. Natl. Acad. Sci. USA* **118**, e2016409118. doi:10.1073/pnas.2016409118

Huang, Y., Cen, L.-P., Choy, K. W., van Rooijen, N., Wang, N., Pang, C. P. and Cui, Q. (2007). JAK/STAT pathway mediates retinal ganglion cell survival after acute ocular hypertension but not under normal conditions. *Exp. Eye Res.* **85**, 684-695. doi:10.1016/j.exer.2007.08.003

Jovanovic, J., Liu, X., Kokona, D., Zinkernagel, M. S. and Ebneter, A. (2020). Inhibition of inflammatory cells delays retinal degeneration in experimental retinal vein occlusion in mice. *Glia* **68**, 574-588. doi:10.1002/glia.23739

Kadye, R., Stoffels, M., Fanucci, S., Mbanxa, S. and Prinsloo, E. (2020). A STAT3 of addiction: adipose tissue, adipocytokine signalling and STAT3 as mediators of metabolic remodelling in the tumour microenvironment. *Cells* **9**, 1043. doi:10.3390/cells9041043

Kanagaraj, P., Chen, J. Y., Skaggs, K., Qadeer, Y., Conner, M., Cutler, N., Richmond, J., Kommidi, V., Poles, A., Affrunti, D. et al. (2020). Microglia stimulate zebrafish brain repair via a specific inflammatory cascade. *bioRxiv* 2020.10.08.330662. doi:10.1101/2020.10.08.330662

Karlstetter, M., Scholz, R., Rutar, M., Wong, W. T., Provis, J. M. and Langmann, T. (2015). Retinal microglia: just bystander or target for therapy? *Prog. Retin. Eye Res.* **45**, 30-57. doi:10.1016/j.preteyeres.2014.11.004

Kassen, S. C., Thummel, R., Campochiaro, L. A., Harding, M. J., Bennett, N. A. and Hyde, D. R. (2009). CNTF induces photoreceptor neuroprotection and Müller glial cell proliferation through two different signaling pathways in the adult zebrafish retina. *Exp. Eye Res.* **88**, 1051-1064. doi:10.1016/j.exer.2009.01.007

Kole, C., Brommer, B., Nakaya, N., Sengupta, M., Bonet-Ponce, L., Zhao, T., Wang, C., Li, W., He, Z. and Tomarev, S. (2020). Activating Transcription Factor 3 (ATF3) protects retinal ganglion cells and promotes functional preservation after optic nerve crush. *Invest. Ophthalmol. Vis. Sci.* **61**, 31. doi:10.1167/iovs.61.2.31

Kölsch, Y., Hahn, J., Sappington, A., Stemmer, M., Fernandes, A. M., Helmbrecht, T. O., Lele, S., Butrus, S., Laurell, E., Arnold-Ammer, I. et al. (2021). Molecular classification of zebrafish retinal ganglion cells links genes to cell types to behavior. *Neuron* **109**, 645-662.e9. doi:10.1016/j.neuron.2020.12.003

Lahne, M., Nagashima, M., Hyde, D. R. and Hitchcock, P. F. (2020). Reprogramming Müller glia to regenerate retinal neurons. *Annu Rev Vis Sci* **6**, 171-193. doi:10.1146/annurev-vision-121219-081808

Langevin, C., Aleksejeva, E., Passoni, G., Palha, N., Levraud, J.-P. and Boudinot, P. (2013). The antiviral innate immune response in fish: evolution and conservation of the IFN system. *J. Mol. Biol.* **425**, 4904-4920. doi:10.1016/j.jmb.2013.09.033

Leach, L. L., Hanovice, N. J., George, S. M., Gabriel, A. E. and Gross, J. M. (2021). The immune response is a critical regulator of zebrafish retinal pigment epithelium regeneration. *Proc. Natl. Acad. Sci. USA* **118**, e2017198118. doi:10.1073/pnas.2017198118

Leibinger, M., Andreadaki, A., Diekmann, H. and Fischer, D. (2013). Neuronal STAT3 activation is essential for CNTF- and inflammatory stimulation-induced CNS axon regeneration. *Cell Death Dis.* **4**, e805. doi:10.1038/cddis.2013.310

Li, L., Huang, H., Fang, F., Liu, L., Sun, Y. and Hu, Y. (2020). Longitudinal morphological and functional assessment of RGC neurodegeneration after optic nerve crush in mouse. *Front. Cell. Neurosci.* **14**, 109. doi:10.3389/fncel.2020.00109

Lin, H., Lee, E., Hestir, K., Leo, C., Huang, M., Bosch, E., Halenbeck, R., Wu, G., Zhou, A., Behrens, D. et al. (2008). Discovery of a cytokine and its receptor by functional screening of the extracellular proteome. *Science* **320**, 807-811. doi:10.1126/science.1154370

Livak, K. J. and Schmittgen, T. D. (2001). Analysis of relative gene expression data using real-time quantitative PCR and the 2−ΔΔCT method. *Methods* **25**, 402-408. doi:10.1006/meth.2001.1262

Luo, J.-M., Cen, L.-P., Zhang, X.-M., Chiang, S. W.-Y., Huang, Y., Lin, D., Fan, Y.-M., Van Rooijen, N., Lam, D. S. C., Pang, C. P. et al. (2007). PI3K/akt, JAK/STAT and MEK/ERK pathway inhibition protects retinal ganglion cells via different mechanisms after optic nerve injury. *Eur. J. Neurosci.* **26**, 828-842. doi:10.1111/j.1460-9568.2007.05718.x

Luo, X., Ribeiro, M., Bray, E. R., Lee, D.-H., Yungher, B. J., Mehta, S. T., Thakor, K. A., Diaz, F., Lee, J. K., Moraes, C. T. et al. (2016). Enhanced transcriptional activity and mitochondrial localization of STAT3 Co-induce axon regrowth in the adult central nervous system. *Cell Rep.* **15**, 398-410. doi:10.1016/j.celrep.2016.03.029

Mac Nair, C. E., Schlamp, C. L., Montgomery, A. D., Shestopalov, V. I. and Nickells, R. W. (2016). Retinal glial responses to optic nerve crush are attenuated in Bax-deficient mice and modulated by purinergic signaling pathways. *J. Neuroinflamm.* **13**, 93. doi:10.1186/s12974-016-0558-y

Mehta, S. T., Luo, X., Park, K. K., Bixby, J. L. and Lemmon, V. P. (2016). Hyperactivated Stat3 boosts axon regeneration in the CNS. *Exp. Neurol.* **280**, 115-120. doi:10.1016/j.expneurol.2016.03.004

Mitchell, D. M., Lovel, A. G. and Stenkamp, D. L. (2018). Dynamic changes in microglial and macrophage characteristics during degeneration and regeneration of the zebrafish retina. *J. Neuroinflamm.* **15**, 163. doi:10.1186/s12974-018-1185-6

Mitchell, D. M., Sun, C., Hunter, S. S., New, D. D. and Stenkamp, D. L. (2019). Regeneration associated transcriptional signature of retinal microglia and macrophages. *Sci. Rep.* **9**, 4768. doi:10.1038/s41598-019-41298-8

Nadal-Nicolás, F. M., Jiménez-López, M., Salinas-Navarro, M., Sobrado-Calvo, P., Vidal-Sanz, M. and Agudo-Barriuso, M. (2017). Microglial dynamics after axotomy-induced retinal ganglion cell death. *J. Neuroinflamm.* **14**, 218. doi:10.1186/s12974-017-0982-7

Osborne, A., Khatib, T. Z., Songra, L., Barber, A. C., Hall, K., Kong, G. Y. X., Widdowson, P. S. and Martin, K. R. (2018). Neuroprotection of retinal ganglion cells by a novel gene therapy construct that achieves sustained enhancement of brain-derived neurotrophic factor/tropomyosin-related kinase receptor-B signaling. *Cell Death Dis.* **9**, 1007. doi:10.1038/s41419-018-1041-8

Park, K., Luo, J.-M., Hisheh, S., Harvey, A. R. and Cui, Q. (2004). Cellular mechanisms associated with spontaneous and ciliary neurotrophic factor-cAMP-induced survival and axonal regeneration of adult retinal ganglion cells. *J. Neurosci.* **24**, 10806-10815. doi:10.1523/JNEUROSCI.3532-04.2004

Park, K. K., Luo, X., Mooney, S. J., Yungher, B. J., Belin, S., Wang, C., Holmes, M. M. and He, Z. (2017). Retinal ganglion cell survival and axon regeneration after optic nerve injury in naked mole-rats. *J. Comp. Neurol.* **525**, 380-388. doi:10.1002/cne.24070

Pittman, A. J., Law, M.-Y. and Chien, C.-B. (2008). Pathfinding in a large vertebrate axon tract: isotypic interactions guide retinotectal axons at multiple choice points. *Development* **135**, 2865-2871. doi:10.1242/dev.025049

Rashid, K., Akhtar-Schaefer, I. and Langmann, T. (2019). Microglia in retinal degeneration. *Front. Immunol.* **10**, 1975. doi:10.3389/fimmu.2019.01975

Sappington, R. M., Chan, M. and Calkins, D. J. (2006). Interleukin-6 protects retinal ganglion cells from pressure-induced death. *Invest. Ophthalmol. Vis. Sci.* **47**, 2932-2942. doi:10.1167/iovs.05-1407

Selvaraj, B. T., Frank, N., Bender, F. L. P., Asan, E. and Sendtner, M. (2012). Local axonal function of STAT3 rescues axon degeneration in the pmn model of motoneuron disease. *J. Cell Biol.* **199**, 437-451. doi:10.1083/jcb.201203109

Shen, S., Niso-Santano, M., Adjemian, S., Takehara, T., Malik, S. A., Minoux, H., Souquere, S., Mariño, G., Lachkar, S., Senovilla, L. et al. (2012). Cytoplasmic STAT3 represses autophagy by inhibiting PKR activity. *Mol. Cell* **48**, 667-680. doi:10.1016/j.molcel.2012.09.013

Sherr, C. J., Rettenmier, C. W., Sacca, R., Roussel, M. F., Look, A. T. and Stanley, E. R. (1985). The c-fms proto-oncogene product is related to the receptor for the mononuclear phagocyte growth factor, CSF-1. *Cell* **41**, 665-676. doi:10.1016/S0092-8674(85)80047-7

Shi, D., Yang, D. and Yan, B. (2010). Dexamethasone transcriptionally increases the expression of the pregnane X receptor and synergistically enhances pyrethroid esfenvalerate in the induction of cytochrome P450 3A23. *Biochem. Pharmacol.* **80**, 1274-1283. doi:10.1016/j.bcp.2010.06.043

Syc-Mazurek, S. B. and Libby, R. T. (2019). Axon injury signaling and compartmentalized injury response in glaucoma. *Prog. Retin. Eye Res.* **73**, 100769. doi:10.1016/j.preteyeres.2019.07.002

Takeda, A., Shinozaki, Y., Kashiwagi, K., Ohno, N., Eto, K., Wake, H., Nabekura, J. and Koizumi, S. (2018). Microglia mediate non-cell-autonomous cell death of retinal ganglion cells. *Glia* **66**, 2366-2384. doi:10.1002/glia.23475

Todd, L., Squires, N., Suarez, L. and Fischer, A. J. (2016). Jak/Stat signaling regulates the proliferation and neurogenic potential of Müller glia-derived progenitor cells in the avian retina. *Sci. Rep.* **6**, 35703. doi.org/10.1038/srep35703

Todd, L., Palazzo, I., Suarez, L., Liu, X., Volkov, L., Hoang, T. V., Campbell, W. A., Blackshaw, S., Quan, N. and Fischer, A. J. (2019). Reactive microglia and IL1β/IL-1R1-signaling mediate neuroprotection in excitotoxin-damaged mouse retina. *J. Neuroinflamm.* **16**, 118. doi:10.1186/s12974-019-1505-5

Tran, N. M., Shekhar, K., Whitney, I. E., Jacobi, A., Benhar, I., Hong, G., Yan, W., Adiconis, X., Arnold, M. E., Lee, J. M. et al. (2019). Single-cell profiles of retinal ganglion cells differing in resilience to injury reveal neuroprotective genes. *Neuron* **104**, 1039-1055.e12. doi:10.1016/j.neuron.2019.11.006

Trevarrow, B., Marks, D. L. and Kimmel, C. B. (1990). Organization of hindbrain segments in the zebrafish embryo. *Neuron* **4**, 669-679. doi:10.1016/0896-6273(90)90194-K

Tsarouchas, T. M., Wehner, D., Cavone, L., Munir, T., Keatinge, M., Lambertus, M., Underhill, A., Barrett, T., Kassapis, E., Ogryzko, N. et al. (2018). Dynamic control of proinflammatory cytokines Il-1β and Tnf-α by macrophages in zebrafish spinal cord regeneration. *Nat. Commun.* **9**, 4670. doi:10.1038/s41467-018-07036-w

Uribe, R. A. and Gross, J. M. (2007). Immunohistochemistry on cryosections from embryonic and adult zebrafish eyes. *CSH Protoc.* **2007**, db.prot4779. doi:10.1101/pdb.prot4779

Van Dyck, A., Bollaerts, I., Beckers, A., Vanhunsel, S., Glorian, N., van Houcke, J., van Ham, T. J., De Groef, L., Andries, L. and Moons, L. (2021). Müller glia-myeloid cell crosstalk accelerates optic nerve regeneration in the adult zebrafish. *Glia*. **69**, 1444-1463. doi:10.1002/glia.23972

Villarino, A. V., Kanno, Y. and O'Shea, J. J. (2017). Mechanisms and consequences of Jak-STAT signaling in the immune system. *Nat. Immunol.* **18**, 374-384. doi:10.1038/ni.3691

Warchol, M. E. (1999). Immune cytokines and dexamethasone influence sensory regeneration in the avian vestibular periphery. *J. Neurocytol.* **28**, 889-900. doi:10.1023/A:1007026306730

White, D. T., Sengupta, S., Saxena, M. T., Xu, Q., Hanes, J., Ding, D., Ji, H. and Mumm, J. S. (2017). Immunomodulation-accelerated neuronal regeneration following selective rod photoreceptor cell ablation in the zebrafish retina. *Proc. Natl. Acad. Sci. USA* **114**, E3719-E3728. doi:10.1073/pnas.1617721114

Williams, P. A., Marsh-Armstrong, N., Howell, G. R. and **Lasker/IRRF Initiative on Astrocytes and Glaucomatous Neurodegeneration Participants**. (2017). Neuroinflammation in glaucoma: a new opportunity. *Exp. Eye Res.* **157**, 20-27. doi:10.1016/j.exer.2017.02.014

Xie, Y., Tolmeijer, S., Oskam, J. M., Tonkens, T., Meijer, A. H. and Schaaf, M. J. M. (2019). Glucocorticoids inhibit macrophage differentiation towards a pro-inflammatory phenotype upon wounding without affecting their migration. *Dis. Model. Mech.* **12**, dmm037887. doi: 10.1242/dmm.037887

Zhao, X.-F., Wan, J., Powell, C., Ramachandran, R., Myers, M. G., Jr and Goldman, D. (2014). Leptin and IL-6 family cytokines synergize to stimulate Müller glia reprogramming and retina regeneration. *Cell Rep.* **9**, 272-284. doi:10.1016/j.celrep.2014.08.047

Zou, S., Tian, C., Ge, S. and Hu, B. (2013). Neurogenesis of retinal ganglion cells is not essential to visual functional recovery after optic nerve injury in adult zebrafish. *PLoS ONE* **8**, e57280. doi:10.1371/journal.pone.0057280